Radiology

ORIGINAL RESEARCH • GASTROINTESTINAL IMAGING

Association of LI-RADS and Histopathologic Features with Survival in Patients with Solitary Resected Hepatocellular Carcinoma

Roberto Cannella, MD • Francesco Matteini, MD • Marco Dioguardi Burgio, MD, PhD • Riccardo Sartoris, MD, PhD • Aurélie Beaufrère, MD, PhD • Julien Calderaro, MD, PhD • Sébastien Mulé, MD, PhD • Edouard Reizine, MD • Alain Luciani, MD, PhD • Alexis Laurent, MD, PhD • Olivier Seror, MD, PhD • Nathalie Ganne-Carrié, MD, PhD • Mathilde Wagner, MD, PhD • Olivier Scatton, MD, PhD • Valérie Vilgrain, MD, PhD • François Cauchy, MD • Christian Hobeika, MD • Maxime Ronot, MD, PhD

From the Section of Radiology, Department of Biomedicine, Neuroscience and Advanced Diagnostics (BiND), University of Palermo, Palermo, Italy (R.C., F.M.); Departments of Radiology (F.M., M.D.B., R.S., V.V., M.R.), Pathology (A.B.), and Hepatobiliary Surgery (F.C., C.H.), Hôpital Beaujon, AP-HP Nord, 100 Blvd du Général Leclerc, 92118 Clichy, France; Université Paris Cité, Paris, France (A.B., V.V., M.R.); Centre de Recherche sur l'Inflammation, INSERM UMR 1149, Paris, France (A.B.); Departments of Pathology (J.C.), Medical Imaging (S.M., E.R., A. Luciani), and Hepatobiliary and Digestive Surgery (A. Laurent), Hôpitaux Universitaires Henri-Mondor, AP-HP, Université Paris Est Créteil, Faculté de Santé, Créteil, France; INSERM U955, Team "Pathophysiology and Therapy of Chronic Viral Hepatitis and Related Cancers," Créteil, France (A. Laurent); Department of Radiology (O. Seror) and Liver Unit (N.G.C.), Avicenne Hospital, AP-HP, Bobigny, France; Sorbonne Paris Nord University, UFR SMBH, Bobigny, France (N.G.C.); INSERM UMR 1138, Team "Functional Genomic of Solid Tumors," Paris, France (N.G.C.); and Departments of Imaging (M.W.) and HPB and Liver Transplantation (O. Scatton), Hôpital Universitaire Pitié-Salpêtrière, AP-HP, Sorbonne Université, Centre de Recherche Saint-Antoine INSERM, Paris, France. Received May 11, 2023; revision requested July 12; final revision received December 30; accepted January 23, 2024. **Address correspondence to** M.R. (email: *maxime.ronot@aphp.fr*).

Conflicts of interest are listed at the end of this article.

See also the editorial by Kartalis and Grigoriadis in this issue.

Radiology 2024; 310(2):e231160 • https://doi.org/10.1148/radiol.231160 • Content codes: GI CT MR

Background: Both Liver Imaging Reporting and Data System (LI-RADS) and histopathologic features provide prognostic information in patients with hepatocellular carcinoma (HCC), but whether LI-RADS is independently associated with survival is uncertain.

Purpose: To assess the association of LI-RADS categories and features with survival outcomes in patients with solitary resected HCC.

Materials and Methods: This retrospective study included patients with solitary resected HCC from three institutions examined with preoperative contrast-enhanced CT and/or MRI between January 2008 and December 2019. Three independent readers evaluated the LI-RADS version 2018 categories and features. Histopathologic features including World Health Organization tumor grade, microvascular and macrovascular invasion, satellite nodules, and tumor capsule were recorded. Overall survival and disease-free survival were assessed with Cox regression models. Marginal effects of nontargetoid features on survival were estimated using propensity score matching.

Results: A total of 360 patients (median age, 64 years [IQR, 56–70 years]; 280 male patients) were included. At CT and MRI, the LI-RADS LR-M category was associated with increased risk of recurrence (CT: hazard ratio [HR] = 1.83 [95% CI: 1.26, 2.66], $P = .001$; MRI: HR = 2.22 [95% CI: 1.56, 3.16], $P < .001$) and death (CT: HR = 2.47 [95% CI: 1.72, 3.55], $P < .001$; MRI: HR = 1.80 [95% CI: 1.32, 2.46], $P < .001$) independently of histopathologic features. The presence of at least one nontargetoid feature was associated with an increased risk of recurrence (CT: HR = 1.80 [95% CI: 1.36, 2.38], $P < .001$; MRI: HR = 1.93 [95% CI: 1.81, 2.06], $P < .001$) and death (CT: HR = 1.51 [95% CI: 1.10, 2.07], $P < .010$) independently of histopathologic features. In matched samples, recurrence was associated with the presence of at least one nontargetoid feature at CT (HR = 2.06 [95% CI: 1.15, 3.66]; $P = .02$) or MRI (HR = 1.79 [95% CI: 1.01, 3.20]; $P = .048$).

Conclusion: In patients with solitary resected HCC, LR-M category and nontargetoid features were negatively associated with survival independently of histopathologic characteristics.

Supplemental material is available for this article.

The Liver Imaging Reporting and Data System (LI-RADS) is an established diagnostic algorithm that is highly specific for the diagnosis of hepatocellular carcinoma (HCC) in high-risk patients with cirrhosis, chronic hepatitis B virus infection, or current or prior HCC history (1,2). Untreated observations are categorized into seven main categories based on their probability of being HCC (LR-1 to LR-5), non-HCC-specific malignant lesions (LR-M), or tumor in vein (LR-TIV) (3,4). In addition to their diagnostic value, LI-RADS categories and features may provide prognostic information (5–8).

Surgical resection and local ablation are the treatment options for patients with single HCC and preserved liver function (4,9). The risk of recurrence after surgical resection remains high, with recurrence in up to 70% of patients within 5 years (4,10). Recent studies have evaluated the prognostic role of LI-RADS features and categories in patients with primary liver carcinoma, including HCC

Abbreviations

DFS = disease-free survival, HCC = hepatocellular carcinoma, HR = hazard ratio, LI-RADS = Liver Imaging Reporting and Data System, OS = overall survival

Summary

Liver Imaging Reporting and Data System LR-M category at CT or MRI as well as histopathologic characteristics were independently associated with survival in patients with solitary resected hepatocellular carcinoma.

Key Results

- In this retrospective study of 360 patients with solitary resected hepatocellular carcinoma, LR-M category at CT and MRI was associated with increased risk of recurrence (HR = 1.83 and 2.22, respectively; $P = .001$ and $P < .001$) and death (HR = 2.47 and 1.80; $P < .001$ for both).
- The presence of at least one nontargetoid feature was independently associated with an increased recurrence risk (CT: HR = 1.80, $P < .001$; MRI: HR = 1.93, $P < .001$).

and other primary non-HCC malignancies (11–14). Disease-free survival (DFS) and overall survival (OS) were found to be shorter in patients with observations categorized as LR-M than in patients with observations categorized as LR-3, LR-4, or LR-5 following surgical resection in Eastern cohorts (11–14). However, histopathologic tumor characteristics such as size, grade, macrovascular and microvascular invasion, satellite nodules, and tumor capsule are also known to be associated with an increased risk of recurrence in patients with resected HCC (15–17). While several LI-RADS imaging features have been associated with clinical outcomes (8,18), whether these imaging features are associated with clinical outcomes in patients with solitary HCC, independently of histopathologic features of tumor aggressiveness, has not been evaluated.

The goal of this study was to assess the association of LI-RADS categories and features and histopathologic tumor features with survival outcomes in patients with solitary HCC undergoing hepatic resection.

Materials and Methods

This retrospective study and chart review were performed according to the Helsinki convention and with approval of the Comité d'Éthique pour la Recherche en Imagerie Médicale (CRM-2211-315). The requirement for informed consent was waived. This study did not receive any support from industrial partners. The authors fully controlled the data and the information submitted for publication.

Study Sample

The medical records of three different academic medical centers (Hôpital Beaujon [Center A], Hôpitaux Universitaires Henri-Mondor [Center B], and Hôpital Universitaire Pitié-Salpêtrière [Center C], France) were searched to select consecutive adult patients who underwent surgical resection for HCC between January 2008 and December 2019. Inclusion criteria for patient selection were as follows: *(a)* surgical resection performed for single HCC, *(b)* complete histopathologic assessment with HCC tumor characteristics available, and *(c)* preoperative contrast-enhanced CT or MRI performed within 3 months before surgery in the absence of any prior treatment. Patients were excluded if *(a)* lesions were found to be non-HCC malignancies at histopathologic analysis (including combined hepatocellular-cholangiocarcinoma), *(b)* more than one HCC was observed at histopathologic analysis, or *(c)* massive bleeding occurred in the tumor.

Patient characteristics including sex, age at surgical resection, risk factors related to chronic liver disease, and the date of recurrence or death were obtained from the medical records by an author who did not participate in the imaging analysis (F.M.). According to the LI-RADS population criteria, patients were considered at high risk of HCC if they had cirrhosis, chronic hepatitis B virus infection, or a prior history of HCC (3). After surgical treatment, patients underwent regular clinical, laboratory, and imaging follow-up according to institutional protocols and clinical requirements. Patients were followed up until December 31, 2021.

This study includes 253 of 277 (91%) previously reported patients (19). The end point of the previous single-center study did not overlap with the outcomes of the current study, as the previous study aimed to describe the imaging features of different HCC subtypes.

Imaging Procedures

Contrast-enhanced CT and MRI examinations were performed with various scanners (16- to 64-row CT scanners; 1.5-T or 3-T MRI scanners) due to the multicenter study design. However, all the included examinations fulfilled LI-RADS technical recommendations (20). The typical MRI protocol included T2-weighted sequences, diffusion-weighted imaging, and dual gradient-echo sequences (in and out of phase). Multiphase contrast-enhanced CT or MRI included precontrast, hepatic arterial (acquired with the bolus tracking technique), portal venous (70–90 seconds), and delayed (180 seconds) phase sequences. Details of CT and MRI systems and contrast agents used are provided in Appendix S1.

Image Evaluation

Three radiologists (M.D.B. [reader 1], R.S. [reader 2], and R.C. [reader 3], with 10, 8, and 6 years of experience in abdominal and liver imaging, respectively) independently reviewed all CT and MRI examinations according to LI-RADS version 2018 criteria (3). Readers were aware of the diagnosis of HCC but blinded to histopathologic and survival data. The CT and MRI examinations were assessed randomly to minimize recall bias. The presence of tumor in vein, LR-M features (both targetoid and nontargetoid), major features, ancillary features favoring malignancy, and ancillary features favoring benignity were assessed according to the LI-RADS version 2018 algorithm and definitions (3).

LI-RADS category was determined at the radiologist's discretion after applying ancillary features and tiebreaking rules for observations both in patients considered to be at high risk according to LI-RADS and in patients not considered to be at high risk (3). We are aware that LI-RADS categories should be applied to diagnose HCC in high-risk patients only. However,

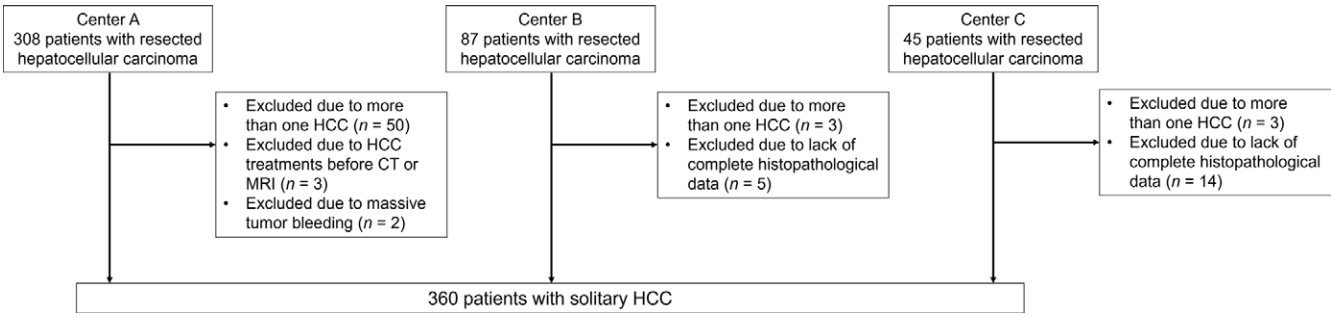

Figure 1: Flowchart of patient selection. HCC = hepatocellular carcinoma.

Table 1: Clinical and Histopathologic Characteristics of the Entire Sample and Patients with Available CT and MRI Examination

Characteristic	All Patients (n = 360)	Patients with CT Examination (n = 300)	Patients with MRI Examination (n = 288)
Age (y)*	64.0 (56.0–70.0)	64.0 (55.3–70.0)	63.5 (56.0–69.0)
Sex			
Male	280 (77.8)	234 (78.0)	225 (78.1)
Female	80 (22.2)	66 (22.0)	63 (21.9)
Age, male patients (y)*	62.5 (54.3–67.8)	63.0 (55.0–70.0)	63.0 (56.0–69.0)
Age, female patients (y)*	66.0 (57.0–70.8)	66.0 (58.5–70.3)	65.0 (55.0–70.0)
Chronic liver disease†			
Hepatitis C virus	110 (30.6)	91 (30.3)	86 (29.9)
Hepatitis B virus	90 (25.0)	75 (25.0)	72 (25.0)
Alcohol abuse	73 (20.3)	60 (20.0)	59 (20.5)
NAFLD	102 (28.3)	85 (28.3)	84 (29.2)
Other	29 (8.1)	25 (8.3)	25 (8.7)
None	26 (7.2)	23 (7.7)	17 (5.9)
Cirrhosis	164 (45.6)	131 (43.7)	134 (46.5)
LI-RADS high-risk status‡	222 (61.7)	180 (60.0)	177 (61.5)
Disease-free survival (mo)§	43.0 (32.2, 53.8)	39.0 (25.7, 52.3)	45.0 (33.4, 56.5)
Overall survival (mo)§	98.0 (84.7, 111.3)	92.0 (79.1, 104.9)	104.0 (83.4, 124.6)
Histopathologic features			
WHO grade			
I	113 (31.4)	93 (31.0)	93 (32.3)
II	219 (60.8)	183 (61.0)	175 (60.8)
III	28 (7.8)	24 (8.0)	20 (6.9)
Macrovascular invasion	35 (9.7)	29 (9.7)	27 (9.4)
Microvascular invasion	172 (47.8)	149 (49.7)	132 (45.8)
Satellite nodules	79 (21.9)	67 (22.3)	61 (21.2)
Tumor capsule	237 (65.8)	201 (67.0)	187 (64.9)
Hepatic fibrosis stage			
F0	29 (8.1)	25 (8.3)	21 (7.3)
F1	39 (10.8)	35 (11.3)	30 (10.4)
F2	53 (14.7)	48 (16.0)	43 (14.9)
F3	75 (20.8)	62 (20.7)	60 (20.8)
F4	164 (45.6)	131 (43.7)	134 (46.5)

Note.—Categorical variables are expressed as numbers of patients, with percentages in parentheses. LI-RADS = Liver Imaging Reporting and Data System, NAFLD = nonalcoholic fatty liver disease, WHO = World Health Organization.

* Continuous variables expressed as medians, with IQRs in parentheses.

† More than one etiology could be present in each patient.

‡ LI-RADS high-risk status was defined as the presence of cirrhosis, chronic hepatitis B virus infection, or a prior history of hepatocellular carcinoma.

§ Continuous variables expressed as medians, with 95% CIs in parentheses.

Table 2: Descriptive Analysis of the Study Samples According to LI-RADS Categories

	Patients with CT Examination (n = 300)				Patients with MRI Examination (n = 288)			
Variable	LR-3–5	LR-M	LR-TIV	*P* Value	LR-3–5	LR-M	LR-TIV	*P* Value
No. of patients	267	15	18		251	24	13	
Age (y)*	64.0 (57.0–70.0)	52.0 (45.0–60.5)	58.5 (54.3–64.8)	.002	64.0 (57.0–70.0)	56.0 (50.8–64.5)	57.0 (54.0–65.0)	.02
Size (mm)*	38.0 (23.0–60.5)	58.0 (34.5–85.5)	97.5 (61.3–123.3)	<.001	34.0 (22.0–55.5)	41.0 (24.5–56.3)	88.0 (60.0–110.0)	<.001
Size > 50 mm	84 (31.5)	8 (53.3)	16 (88.9)	<.001	71 (28.3)	9 (37.5)	11 (84.6)	<.001
Medical center				.55				.65
A	198 (74.2)	13 (86.7)	15 (83.3)		175 (69.7)	15 (62.5)	11 (84.6)	
B	50 (18.7)	2 (13.3)	3 (16.7)		55 (21.9)	7 (29.2)	2 (15.4)	
C	19 (7.1)	0 (0.0)	0 (0.0)		21 (8.4)	2 (8.3)	0 (0.0)	
LI-RADS high-risk status†	161 (60.3)	10 (66.7)	9 (50.0)	.60	151 (60.2)	19 (79.2)	7 (53.8)	.16
Male sex	206 (77.2)	14 (93.3)	14 (77.8)	.34	195 (77.7)	19 (79.2)	11 (84.6)	.84
Satellite nodules	52 (19.5)	7 (46.7)	8 (44.4)	.003	44 (17.5)	9 (37.5)	8 (61.5)	<.001
Microvascular invasion	117 (43.8)	14 (93.3)	18 (100.0)	<.001	104 (41.4)	15 (62.5)	13 (100.0)	<.001
Macrovascular invasion	11 (4.1)	2 (13.3)	16 (88.9)	<.001	12 (4.8)	2 (8.3)	13 (100.0)	<.001
Tumor capsule	189 (70.8)	8 (53.3)	4 (22.2)	<.001	171 (68.1)	13 (54.2)	3 (23.1)	.002
WHO grade				.002				<.001
I	89 (33.3)	2 (13.3)	2 (11.1)		88 (35.1)	4 (16.7)	1 (7.7)	
II	162 (60.7)	10 (66.7)	11 (61.1)		152 (60.6)	16 (66.7)	7 (53.8)	
III	16 (6.0)	3 (20.0)	5 (27.8)		11 (4.4)	4 (16.7)	5 (38.5)	
At least one LR-M feature	63 (23.6)	15 (100.0)	16 (88.9)	<.001	56 (22.3)	22 (91.7)	10 (76.9)	<.001
At least one targetoid feature	1 (0.4)	5 (33.3)	0 (0.0)	<.001	1 (0.4)	16 (66.7)	1 (7.7)	<.001
At least one nontargetoid feature	62 (23.2)	11 (73.3)	16 (88.9)	<.001	55 (21.9)	12 (50.0)	10 (76.9)	<.001

Note.—Categorical variables are expressed as numbers of patients, with percentages in parentheses, and were compared using Pearson χ^2 test or Fisher exact test, as appropriate. LI-RADS = Liver Imaging Reporting and Data System, WHO = World Health Organization.

* Continuous variables are expressed as medians, with IQRs in parentheses, and were compared using the Kruskal-Wallis test.

† LI-RADS high-risk status was defined as the presence of cirrhosis, chronic hepatitis B virus infection, or a prior history of hepatocellular carcinoma.

the current study assesses the prognostic rather than the diagnostic value of LI-RADS. Thus, a final LI-RADS category was intentionally determined for all observations assuming that the HCC diagnosis had been made before applying the LI-RADS algorithm, to explore the prognostic value of the system. According to LI-RADS version 2018, observations with nontargetoid features were categorized as LR-M if they did not meet LR-5 or LR-TIV criteria (3). For binary features (eg, nonrim arterial phase hyperenhancement), the feature was considered present if it was reported by at least two of the three readers. In cases of disagreement on LI-RADS category, a consensus reassessment was performed to determine the final LI-RADS category.

Histopathologic Analysis

Expert liver pathologists (A.B. and J.C.) assessed resected specimens and hematoxylin-eosin-saffron–stained slides of each tumor at each referral center. The following macroscopic and microscopic features were assessed in each patient: differentiation grade (World Health Organization grade) (21), microvascular invasion (presence of clusters of tumor cells in vessels located in the tumor capsule or in the surrounding nontumoral liver identified during microscopic examination without being seen during macroscopic examination), macrovascular invasion (presence of tumor in vessels located in the tumor capsule or in the surrounding nontumoral liver identified during macroscopic examination), satellite nodules (nodules smaller than 2 cm and located less than 2 cm from the main tumor), and tumor capsule (presence of fibrous tissue surrounding the nodule and separating it from the adjacent liver parenchyma).

The stage of fibrosis in the nontumoral liver was evaluated according to the METAVIR (Meta-analysis of Histological Data

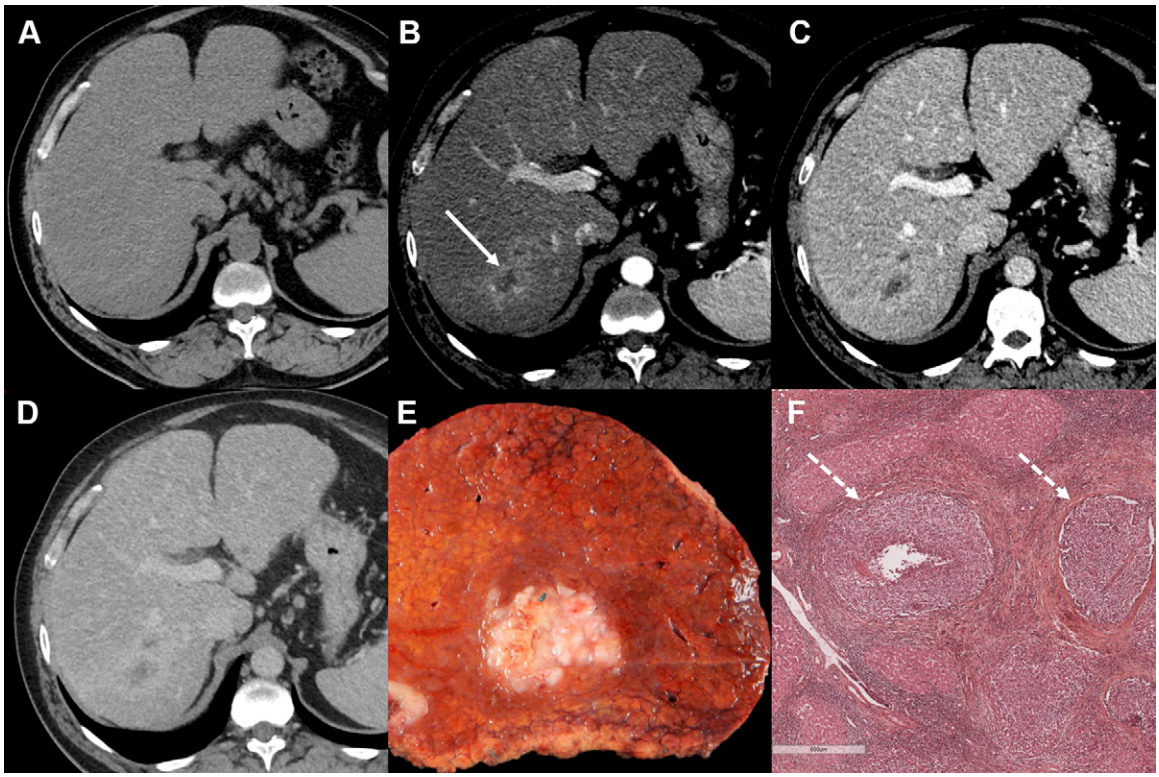

Figure 2: Images in a 55-year-old male patient with a history of hepatitis C virus–related cirrhosis and a 45-mm hepatocellular carcinoma (HCC). Axial **(A)** precontrast and **(B–D)** contrast-enhanced CT images in the **(B)** hepatic arterial, **(C)** portal venous, and **(D)** delayed phases show lesion (arrow in **B**) with rim arterial phase hyperenhancement categorized as Liver Imaging Reporting and Data System category LR-M. **(E)** Photograph of resected specimen shows a poorly demarcated HCC. **(F)** Photomicrograph (hematoxylin-eosin stain) reveals a poorly differentiated HCC with microvascular invasion (arrows). Scale bar in **F** = 600 μm. Intrahepatic recurrence was observed at 14 months after resection.

in Viral Hepatitis) staging system (22) and the system of Kleiner et al (23) in patients with metabolic syndrome.

Statistical Analyses

Continuous data are expressed as medians and IQRs or medians and 95% CIs and were compared using the Kruskal-Wallis test. Categorical data are expressed as percentages and were compared using Pearson χ^2 test or Fisher exact test, as appropriate. The Fleiss κ test and the intraclass correlation coefficient (ICC) with an absolute agreement with the two-way mixed-effects model were calculated to evaluate interreader agreement on LI-RADS features and size, respectively. Agreement was categorized as poor (κ < 0.00), slight (κ = 0.00–0.20), fair (κ = 0.21–0.40), moderate (κ = 0.41–0.60), substantial (κ = 0.61–0.80), or almost perfect (κ = 0.81–1.00) for Fleiss κ and as poor (ICC < 0.50), moderate (ICC = 0.50–0.75), good (ICC = 0.75–0.90), or excellent (ICC > 0.90) for ICC (24).

OS was defined as the interval between surgical resection and all-cause death. DFS was defined as the interval between curative-intent surgical resection and tumor recurrence (intrahepatic or extrahepatic). All multivariable analyses were complete case (ie, they included patients without missing data). Right-censored outcomes (ie, OS and DFS) were quantified using Cox proportional hazards regression models to estimate conditional effects (ie, average effect of exposure on the individual; estimated effect sizes are expressed as hazard ratios [HRs] with 95% CIs) with medical center–specific cluster-robust variance (25–27). Survival probabilities were computed using the Kaplan-Meier estimate and compared using the log-rank test. Variables included in models were chosen based on their clinical relevance (ie, acknowledged prognostic factors after HCC resection). All regressions underwent convergence and singularity checking. The proportional hazards assumption for Cox models was checked using Schoenfeld residuals.

A model of exposure was estimated using 4:1 nearest neighbor matching without replacement using propensity score distance (estimated with logistic regression) and a caliper less than 0.1 (Matchit package in R) to estimate the marginal effect (ie, average effect of exposure on the population; estimated effect sizes are expressed as HRs with 95% CIs) of being exposed to at least one nontargetoid feature (28,29). Covariates included in the propensity score estimation were chosen based on clinical relevance and their imbalance regarding the matching variable of interest. Covariate balance before and after matching was estimated using standardized mean differences.

The marginal HRs in the matched samples were estimated using a weighted (incorporating the matching weights) Cox model without covariates (ie, noncollapsible HRs) with clustered variance on matching pair membership (cluster-robust standard errors).

Statistical significance testing was two-sided. $P < .05$ was considered statistically significant for all tests. There were no

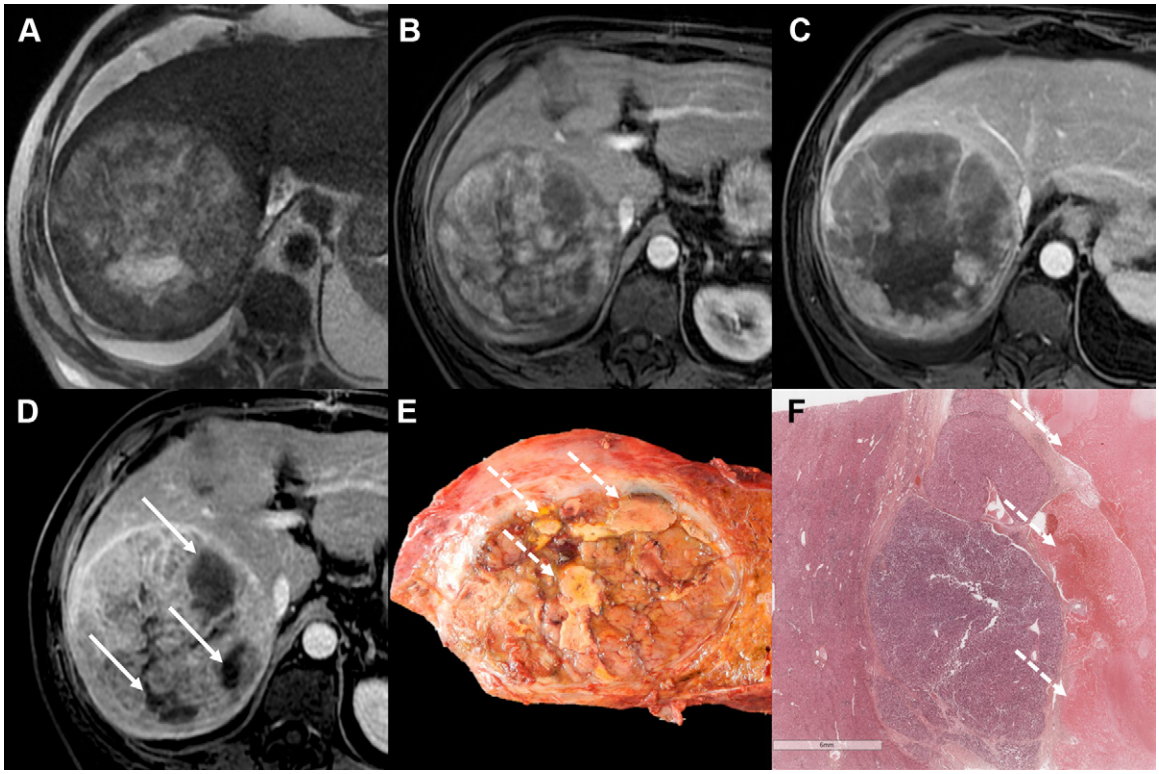

Figure 3: Images in a 66-year-old male patient with a history of cirrhosis and a 140-mm hepatocellular carcinoma (HCC). Axial **(A)** T2-weighted and **(B–D)** contrast-enhanced MRI scans in the **(B)** hepatic arterial, **(C)** portal venous, and **(D)** delayed phases show a lesion categorized as Liver Imaging Reporting and Data System category LR-5 with nonrim arterial phase hyperenhancement, nonperipheral "washout," enhancing "capsule," and necrosis or severe ischemia (nontargetoid feature; arrows in **D**). **(E)** Photograph and **(F)** photomicrograph (hematoxylin-eosin stain) of the resected specimen show an encapsulated HCC with areas of internal necrosis (arrows). Scale bar in **F** = 6 mm. Intrahepatic recurrence was observed at 39 months after resection.

missing values. All statistical analyses were performed by one author (C.H.) using R version 4.2.0 (R Foundation for Statistical Computing) with the survival package.

Results

Characteristics of Patients and HCCs

The initial study sample included 486 patients. Patients were excluded if *(a)* they had more than one HCC at histopathologic analysis (n = 56); *(b)* there was no available preoperative contrast-enhanced CT and/or MRI examination (n = 46); *(c)* they were treated before the imaging examination (n = 3); *(d)* complete histopathologic data were not available (n = 19); or *(e)* massive bleeding occurred in the tumor (n = 2) (Fig 1). The final cohort included 360 patients (median age, 64 years [IQR, 56–70 years]; 280 male patients and 80 female patients) with solitary resected HCC (Fig 1). Hepatitis C was the most common cause of underlying chronic liver disease (110 of 360 [30.6%] patients). Only 66.4% (239 of 360) of patients had advanced fibrosis, including 164 of 360 (45.6%) patients with cirrhosis. The clinical and histopathologic features of the patients and HCCs are provided in Table 1.

Contrast-enhanced CT examinations were available in 300 of 360 (83.3%) patients, and contrast-enhanced MRI examinations were available in 288 of 360 (80.0%) patients.

LI-RADS Categories at CT and MRI

LI-RADS–defined high-risk criteria were present in 222 of 360 (61.7%) patients. LI-RADS imaging features and categories by reader, and interreader agreement, for contrast-enhanced CT and MRI examinations are reported in Tables S1 and S2, respectively; intramodality differences are reported in Table S3. Descriptive analyses of patients in the CT and MRI study samples according to LI-RADS categories are displayed in Table 2. Of the 300 observations in patients who underwent contrast-enhanced CT, the numbers of observations in each consensus LI-RADS category were as follows: LR-3, 10 (3.3%); LR-4, 33 (11%); LR-5, 224 (74.7%); LR-M, 15 (5%); and LR-TIV, 18 (6%). The interreader agreement was moderate for LI-RADS category (κ = 0.58 [95% CI: 0.58, 0.58]) and substantial for the presence of at least one LR-M feature (κ = 0.67 [95% CI: 0.67, 0.68]). Of the 288 observations in patients who underwent contrast-enhanced MRI, the numbers of observations in each consensus LI-RADS category were as follows: LR-3, two (0.7%); LR-4, 25 (8.7%); LR-5, 224 (77.8%); LR-M, 24 (8.3%); and LR-TIV, 13 (4.5%) The interreader agreement was substantial for LI-RADS category (κ = 0.62 [95% CI: 0.62, 0.62]) and for the presence of at least one LR-M feature (κ = 0.64 [95% CI: 0.64, 0.64]). Figures 2 and 3 show example images in a patient who underwent CT examination and a patient who underwent MRI examination, respectively.

Table 3: Univariable and Multivariable Cox Models with Medical Center–Specific Robust Variance for Recurrence and All-Cause Death in the CT and MRI Samples

	Recurrence				Death			
	CT		MRI		CT		MRI	
Variable	Hazard Ratio	*P* Value	Hazard Ratio	*P* Value	Hazard Ratio	*P* Value	Hazard Ratio	*P* Value
Univariable analyses								
LR-5	Ref		Ref		Ref		Ref	
LR-3 or -4	0.98 (0.61, 1.57)	.94	0.90 (0.51, 1.57)	.70	1.42 (0.82, 2.46)	.21	0.85 (0.41, 1.79)	.67
LR-M	2.15 (1.59, 2.90)	<.001	2.61 (1.62, 4.19)	<.001	3.06 (1.76, 5.31)	<.001	1.75 (1.29, 2.38)	<.001
LR-TIV	1.82 (1.20, 2.77)	.005	1.66 (1.31, 2.10)	<.001	1.58 (1.11, 2.24)	.01	2.22 (1.61, 3.05)	<.001
Multivariable analyses								
LI-RADS category								
LR-3–5	Ref		Ref		Ref		Ref	
LR-M	1.83 (1.26, 2.66)	.001	2.22 (1.56, 3.16)	<.001	2.47 (1.72, 3.55)	<.001	1.80 (1.32, 2.46)	<.001
LR-TIV	0.71 (0.46, 1.08)	.11	0.72 (0.56, 0.92)	.009	0.70 (0.41, 1.20)	.19	1.04 (0.86, 1.27)	.66
LI-RADS high-risk status*	1.35 (1.24, 1.47)	<.001	1.13 (1.01, 1.27)	.04	0.95 (0.83, 1.08)	.42	0.65 (0.40, 1.07)	.09
Size (mm)†								
<Q1	1.01 (0.83, 1.23)	.93	0.90 (0.71, 1.13)	.36	1.64 (1.14, 2.36)	.008	1.06 (0.81, 1.38)	.68
Q1–Q3	1.26 (1.06, 1.49)	.007	0.95 (0.67, 1.34)	.75	2.05 (1.09, 3.86)	.03	1.21 (0.79, 1.83)	.38
>Q3	2.62 (2.50, 2.74)	<.001	2.02 (1.27, 3.21)	.003	3.11 (2.19, 4.42)	<.001	1.82 (1.08, 3.05)	.03
Age (y)‡								
<Q1	1.38 (1.22, 1.57)	<.001	0.90 (0.51, 1.57)	.70	1.54 (1.16, 2.05)	.003	1.10 (0.87, 1.38)	.42
Q1–Q3	1.43 (1.25, 1.63)	<.001	0.87 (0.50, 1.52)	.63	1.56 (1.09, 2.23)	.014	1.04 (0.78, 1.39)	.77
>Q3	1.23 (1.07, 1.41)	.003	0.86 (0.53, 1.41)	.56	1.48 (0.97, 2.25)	.07	1.28 (1.26, 1.29)	<.001
Male sex	1.47 (0.99, 2.16)	.05	1.84 (1.35, 2.52)	<.001	2.02 (1.19, 3.41)	.009	2.43 (1.43, 4.11)	<.001
Satellite nodules	1.12 (0.85, 1.47)	.42	1.19 (0.95, 1.48)	.13	1.28 (1.19, 1.37)	<.001	0.98 (0.66, 1.47)	.94
Microvascular invasion	1.30 (0.83, 2.04)	.25	1.39 (1.23, 1.57)	<.001	1.20 (0.58, 2.48)	.63	1.39 (0.97, 1.99)	.08
WHO grade								
I	Ref		Ref		Ref		Ref	
II	1.10 (0.69, 1.75)	.69	1.06 (0.93, 1.20)	.38	1.36 (0.95, 1.94)	.09	1.56 (1.33, 1.82)	<.001
III	1.55 (0.88, 2.72)	.13	1.09 (0.35, 3.44)	.88	3.07 (1.68, 5.61)	<.001	2.36 (0.80, 6.92)	.12

Note.—Data in parentheses are 95% CIs. Time to recurrence and time to death were right-censored response variables. LI-RADS = Liver Imaging Reporting and Data System, Q1 = quartile 1, Q3 = quartile 3, Ref = reference, WHO = World Health Organization.

* LI-RADS high-risk status was defined as the presence of cirrhosis, chronic hepatitis B virus infection, or a prior history of hepatocellular carcinoma.

† For tumor size, Q1 and Q3 thresholds are 25 and 70 mm for CT examinations and 25 and 60 mm for MRI examinations.

‡ For age, Q1 and Q3 thresholds are 55 and 70 years for both CT and MRI examinations.

LI-RADS Categories Associated with Survival

The median follow-up times were 56 months (95% CI: 51, 61) and 56 months (95% CI: 52, 62) in the CT and MRI samples, respectively.

Univariable Cox models (Table 3) with LR-5 as the reference category showed that the LR-M category (CT: HR = 2.15 [95% CI: 1.59, 2.90], $P < .001$; MRI: HR = 2.61 [95% CI: 1.62, 4.19], $P < .001$) and LR-TIV category (CT: HR = 1.82 [95% CI: 1.20, 2.77], $P = .005$; MRI: HR = 1.66 [95% CI: 1.31, 2.10], $P < .001$) were associated with increased risk of recurrence in both the CT and MRI samples.

The LR-M and LR-TIV categories were associated with histopathologic features related to poor prognosis (Table 2). A multivariable Cox model (Table 3) showed that the LR-M category was associated with increased risk of recurrence (CT: HR = 1.83 [95% CI: 1.26, 2.66], $P = .001$; MRI: HR = 2.22 [95% CI: 1.56, 3.16], $P < .001$) and death (CT: HR = 2.47 [95% CI: 1.72, 3.55], $P < .001$; MRI: HR = 1.80 [95% CI: 1.32, 2.46], $P < .001$), independently of these histopathologic features.

LR-M, Targetoid, and Nontargetoid Features

In the CT and MRI samples, 94 of 300 (31.3%) and 88 of 288 (30.1%) patients, respectively, had tumors displaying at least one LR-M feature. Among them, at least one targetoid feature was observed in six of 94 (6.4%) and 18 of 88 (20.5%) patients, and at least one nontargetoid feature was observed in

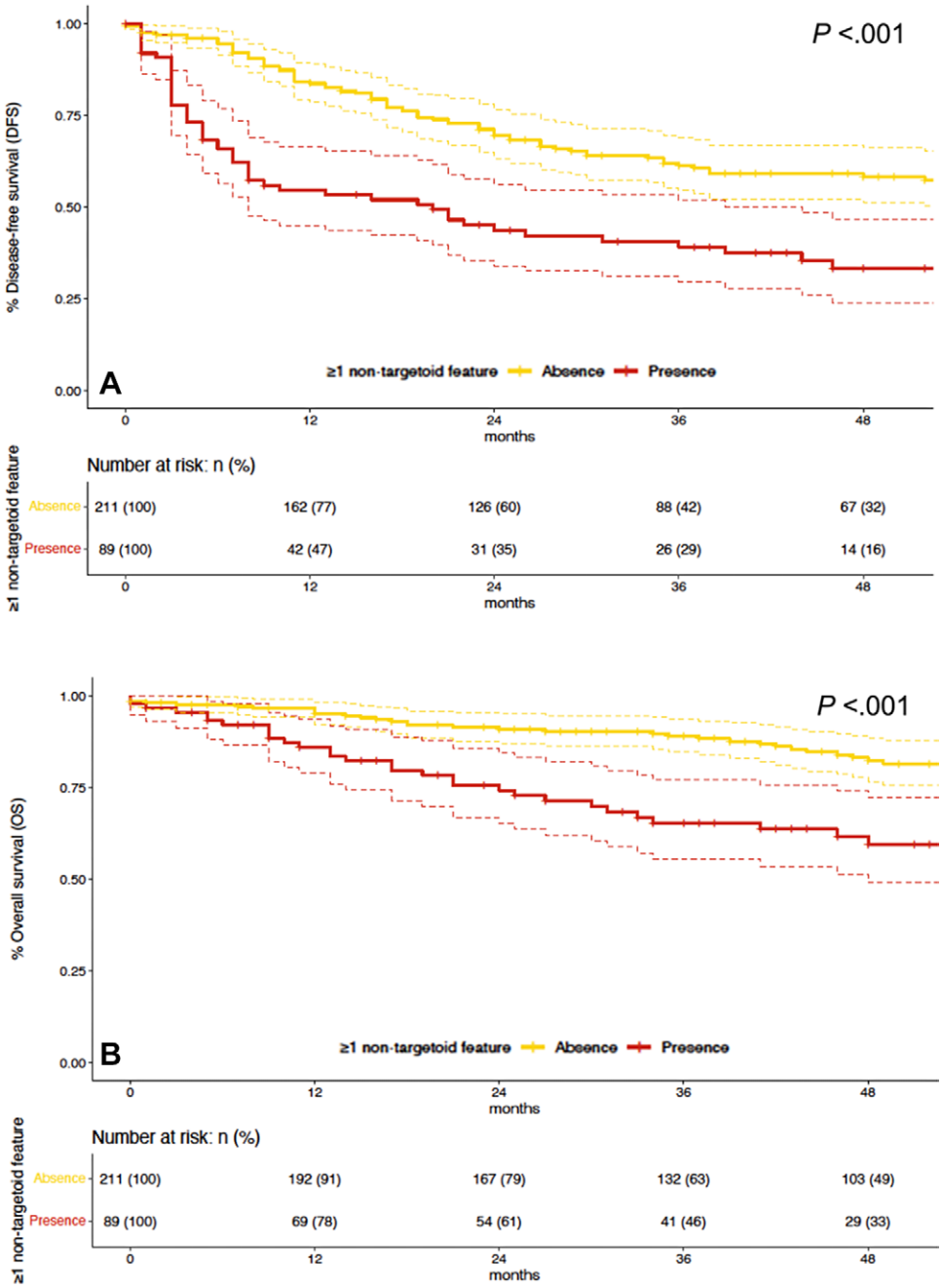

Figure 4: Graphs show crude Kaplan-Meier curves for **(A)** disease-free survival (DFS) and **(B)** overall survival (OS) in patients with CT examinations according to the presence of at least one nontargetoid feature *(Fig 4 continues).*

89 of 94 (94.7%) and 77 of 88 (87.5%) patients, respectively. Over 60% of observations with at least one LR-M feature were classified as LR-5, and 67.4% and 70.1% of observations with at least one nontargetoid feature were classified as LR-5 in the CT and MRI samples, respectively. The comparative analysis of patients with and without at least one LR-M feature is shown in Table S4.

Influence of Nontargetoid Features on Survival

Crude DFS (log-rank test, $P < .001$ for both CT and MRI samples) and OS (log-rank test, $P < .001$ for CT sample and $P = .03$ for MRI sample) were decreased in patients with at least one nontargetoid feature compared with patients without nontargetoid features (Fig 4). The comparative analysis between patients with and without at least one nontargetoid feature is displayed in Table 4. A multivariable Cox model (Table 5) showed that the presence of at least one nontargetoid feature was independently associated with an increased risk of recurrence (CT: HR = 1.80 [95% CI: 1.36, 2.38], $P < .001$; MRI: HR = 1.93 [95% CI: 1.81, 2.06], $P < .001$). The presence of at least one nontargetoid feature was also associated with an increased risk of death in the CT sample (HR = 1.51 [95% CI: 1.10, 2.07]; $P = .01$).

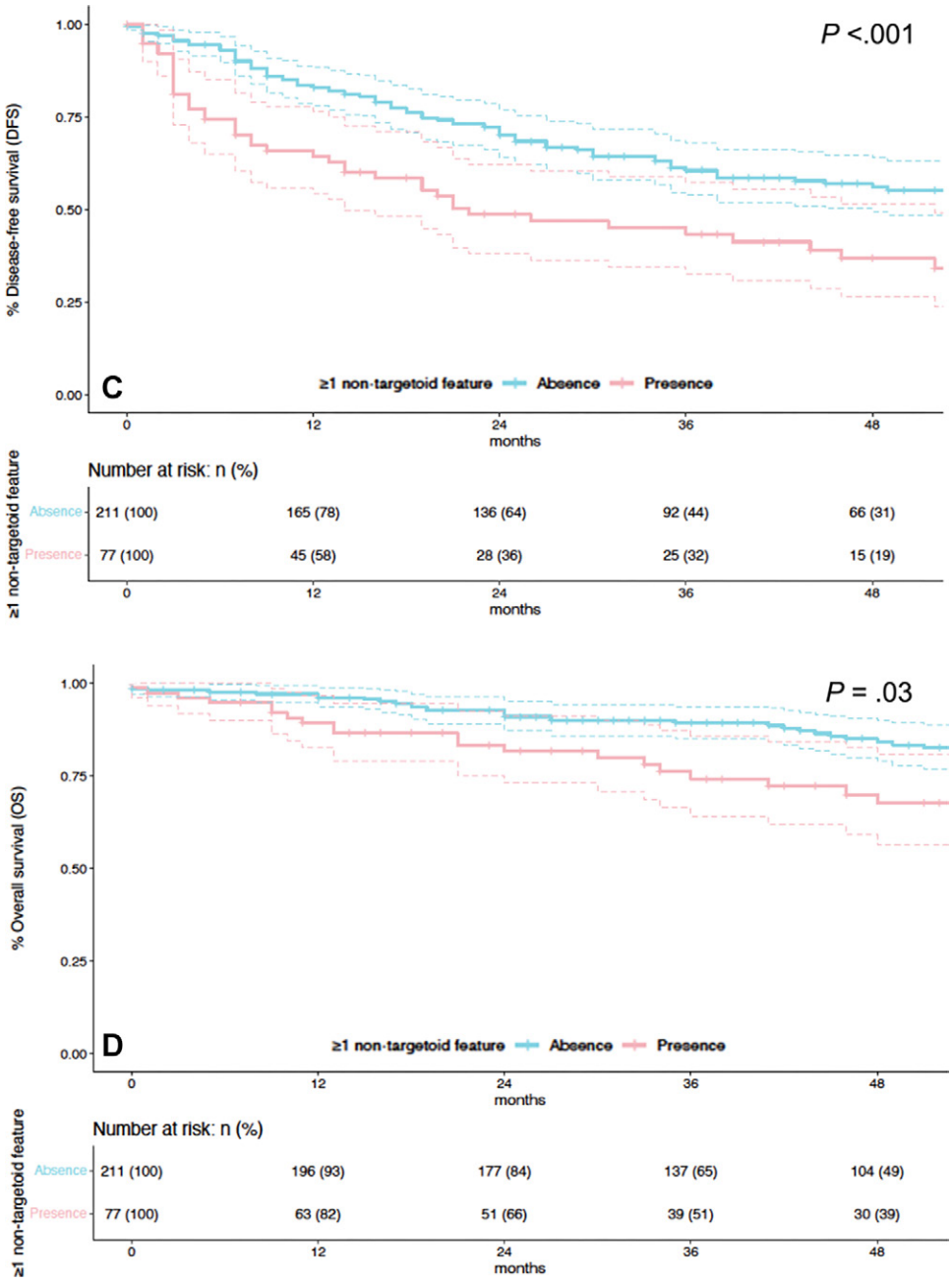

Figure 4 *(continued).* Graphs show crude Kaplan-Meier curves for **(C)** DFS and **(D)** OS in patients with MRI examinations according to the presence of at least one nontargetoid feature.

Marginal Effect of Nontargetoid Features on Survival

Patients with and without at least one nontargetoid feature were matched (matching specifications are displayed in Table S5) in the CT and MRI samples to balance the following covariables: medical center, size greater than 50 mm, LI-RADS high-risk status, satellite nodules, micro- and macrovascular invasion, World Health Organization grade, and LI-RADS category. In the CT sample, 42 patients with at least one nontargetoid feature were matched to 74 patients without nontargetoid features. In the MRI sample, 41 patients with at least one nontargetoid feature were matched to 75 patients without nontargetoid features.

The marginal HR of recurrence associated with the presence of at least one nontargetoid feature in the CT and MRI matched samples was 2.06 (95% CI: 1.15, 3.66; $P = .02$) and 1.79 (95% CI: 1.01, 3.20; $P = .048$), respectively. The marginal HR of death associated with the presence of at least one nontargetoid feature in the CT and MRI matched samples was 2.72 (95% CI: 1.20, 6.14; $P = .02$) and 1.06 (95% CI: 0.51, 2.24; $P = .87$), respectively. Survival curves after matching are displayed in Figure 5.

Discussion

Recent data have validated the role of the Liver Imaging Reporting and Data System (LI-RADS) algorithm for diagnosing

Table 4: Comparative Analysis of Patients with and without Nontargetoid Features in the CT and MRI Samples

Variable	Patients with CT Examination (n = 300)			Patients with MRI Examination (n = 288)		
	Without Nontargetoid Features	With Nontargetoid Features	*P* Value	Without Nontargetoid Features	With Nontargetoid Features	*P* Value
No. of patients	211	89		211	77	
Age (y)*	64.0 (56.0–70.0)	64.0 (55.0–70.0)	.90	63.0 (56.5–69.0)	64.0 (54.0–70.0)	.56
Size (mm)*	32.0 (21.0–43.0)	90.0 (60.0–135.0)	<.001	29.0 (20.0–40.5)	81.0 (55.0–122.0)	<.001
Size > 50 mm	35 (16.6)	73 (82.0)	<.001	28 (13.3)	63 (81.8)	<.001
Medical center			.001			.008
A	147 (69.7)	79 (88.8)		137 (64.9)	64 (83.1)	
B	45 (21.3)	10 (11.2)		56 (26.5)	8 (10.4)	
C	19 (9.0)	0 (0.0)		18 (8.5)	5 (6.5)	
LI-RADS high-risk status†	140 (66.4)	40 (44.9)	.001	140 (66.4)	37 (48.1)	.007
Male sex	165 (78.2)	69 (77.5)	>.99	166 (78.7)	59 (76.6)	.83
Satellite nodules	33 (15.6)	34 (38.2)	<.001	35 (16.6)	26 (33.8)	.003
Microvascular invasion	90 (42.7)	59 (66.3)	<.001	86 (40.8)	46 (59.7)	.006
Macrovascular invasion	8 (3.8)	21 (23.6)	<.001	12 (5.7)	15 (19.5)	.001
Tumor capsule	142 (67.3)	59 (66.3)	.97	134 (63.5)	53 (68.8)	.46
WHO grade			.003			.02
I	76 (36.0)	17 (19.1)		75 (35.5)	18 (23.4)	
II	123 (58.3)	60 (67.4)		126 (59.7)	49 (63.6)	
III	12 (5.7)	12 (13.5)		10 (4.7)	10 (13.0)	
LI-RADS category			<.001			<.001
LR-3	10 (4.7)	0 (0.0)		2 (0.9)	0 (0.0)	
LR-4	31 (14.7)	2 (2.2)		24 (11.4)	1 (1.3)	
LR-5	164 (77.7)	60 (67.4)		170 (80.6)	54 (70.1)	
LR-M	4 (1.9)	11 (12.4)		12 (5.7)	12 (15.6)	
LR-TIV	2 (0.9)	16 (18.0)		3 (1.4)	10 (13.0)	
At least one LR-M feature	5 (2.4)	89 (100.0)	<.001	11 (5.2)	77 (100.0)	<.001
At least one targetoid feature	4 (1.9)	2 (2.2)	>.99	10 (4.7)	8 (10.4)	.14
At least one nontargetoid feature	0 (0.0)	89 (100.0)	<.001	0 (0.0)	77 (100.0)	<.001

Note.—Categorical variables are expressed as numbers of patients, with percentages in parentheses, and were compared using Pearson χ^2 test or Fisher exact test, as appropriate. LI-RADS = Liver Imaging Reporting and Data System, WHO = World Health Organization.

* Continuous variables are expressed as medians, with IQRs in parentheses, and were compared using the Kruskal-Wallis test.

† LI-RADS high-risk status was defined as the presence of cirrhosis, chronic hepatitis B virus infection, or a prior history of hepatocellular carcinoma.

hepatocellular carcinoma and have shown that different LI-RADS categories and imaging features have potential prognostic value. In the current study, observations categorized as LR-M were associated with lower overall and disease-free survival. Importantly, while LR-M observations were found to have more frequent negative histoprognostic features (higher World Health Organization grade, greater frequency of microvascular and macrovascular invasion, satellite nodules, less frequent tumor capsule), the LR-M category was shown to bear independent prognostic value. Moreover, the presence of at least one nontargetoid feature was independently associated with an increased recurrence risk (CT: hazard ratio [HR] = 1.80 [95% CI: 1.36, 2.38], $P < .001$; MRI: HR = 1.93 [95% CI: 1.81, 2.06], $P < .001$), regardless of the LI-RADS category.

Our results support prior studies (13,14) showing a poorer prognosis with LR-M category tumors after surgical resection in patients with solitary HCCs. In a single-center study including 281 HCCs in patients who underwent contrast-enhanced MRI, Shin et al (13) reported that tumor size of 3 cm or greater and LR-M category were independently associated with early HCC recurrence after resection. Choi et al (12) also showed that in patients with cirrhosis undergoing surgical resection of primary liver cancers, the LR-M category at preoperative imaging predicted shorter overall survival and recurrence-free survival relative to the LR-4 or LR-5 categories. Importantly, most studies have focused on the value of targetoid LR-M features, especially rim arterial phase hyperenhancement. For instance, Moon et al (14) reported that LR-M observations with rim arterial phase hyperenhancement were associated with shorter OS and DFS in patients, while no difference in survival was observed between LR-4 or LR-5 and LR-M category observations without rim arterial phase hyperenhancement (14).

Table 5: Multivariable Cox Models with Medical Center–Specific Robust Variance for Recurrence and Death in the CT and MRI Samples

	Recurrence				Death			
	CT		MRI		CT		MRI	
Variable	Hazard Ratio	*P* Value	Hazard Ratio	*P* Value	Hazard Ratio	*P* Value	Hazard Ratio	*P* Value
At least one nontargetoid feature	1.80 (1.36, 2.38)	<.001	1.93 (1.81, 2.06)	<.001	1.51 (1.10, 2.07)	.01	1.05 (0.69, 1.60)	.83
At least one targetoid feature	0.93 (0.84, 1.03)	.18	1.59 (0.73, 3.49)	.24	1.21 (1.01, 1.43)	.04	1.53 (0.96, 2.41)	.07
LI-RADS high-risk status*	1.34 (1.29, 1.39)	<.001	1.10 (0.92, 1.32)	.29	0.93 (0.80, 1.07)	.29	0.64 (0.43, 0.96)	.03
Size (mm)†								
<Q1		.45		.32		.05		.74
Q1–Q3	1.01 (0.89, 1.14)	.94	0.75 (0.52, 1.08)	.12	1.61 (0.89, 2.90)	.11	1.14 (0.75, 1.74)	.54
>Q3	1.46 (1.28, 1.65)	<.001	1.02 (0.62, 1.66)	.95	1.78 (1.50, 2.10)	<.001	1.62 (1.02, 2.55)	.04
Age (y)‡								
<Q1		<.001		.26		.005		.03
Q1–Q3	1.27 (1.10, 1.46)	<.001	0.75 (0.46, 1.23)	.26	1.50 (1.04, 2.16)	.03	1.04 (0.94, 1.15)	.47
>Q3	1.06 (0.92, 1.23)	.43	0.75 (0.50, 1.12)	.16	1.41 (0.92, 2.15)	.12	1.25 (1.03, 1.52)	.02
Male sex	1.45 (0.97, 2.16)	.07	1.78 (1.26, 2.51)	<.001	2.14 (1.32, 3.47)	.002	2.40 (1.49, 3.87)	<.001
Satellite nodules	0.99 (0.73, 1.36)	.97	1.13 (0.91, 1.40)	.28	1.16 (1.07, 1.24)	<.001	0.93 (0.59, 1.46)	.75
Microvascular invasion	1.42 (0.98, 2.06)	.07	1.40 (1.09, 1.80)	.009	1.27 (0.61, 2.65)	.52	1.33 (0.88, 2.02)	.18
Macrovascular invasion	0.90 (0.79, 1.03)	.13	1.23 (0.66, 2.28)	.52	1.02 (0.81, 1.30)	.84	1.50 (1.07, 2.09)	.02
WHO grade								
I	Ref		Ref		Ref		Ref	
II	1.05 (0.65, 1.69)	.85	1.07 (0.84, 1.36)	.59	1.31 (0.87, 1.98)	.19	1.56 (1.34, 1.80)	<.001
III	1.37 (0.88, 2.14)	.16	0.90 (0.29, 2.77)	.85	2.70 (1.60, 4.55)	<.001	2.18 (0.76, 6.23)	.15

Note.—Data in parentheses are 95% CIs. Time to recurrence and time to death were right-censored response variables. LI-RADS = Liver Imaging Reporting and Data System, Q1 = quartile 1, Q3 = quartile 3, Ref = reference, WHO = World Health Organization.

* LI-RADS high-risk status was defined as the presence of cirrhosis, chronic hepatitis B virus infection, or a prior history of hepatocellular carcinoma.

† For tumor size, Q1 and Q3 thresholds are 25 and 70 mm for CT examinations and 25 and 60 mm for MRI examinations.

‡ For age, Q1 and Q3 thresholds are 55 and 70 years for both CT and MRI examinations.

The LR-M category and LR-M features including rim arterial phase hyperenhancement have been associated with negative histoprognostic features such as microvascular invasion or poorer tumor differentiation (8,30). Therefore, one may hypothesize that the prognostic value of the LR-M category is but the reflection of the pathologic phenotype of tumors. In the current study, differences in OS or DFS were observed when patients were stratified by several histopathologic features, such as World Health Organization grade, microvascular invasion, and satellite nodules. However, the multivariable analysis including imaging and pathologic characteristics confirmed that the LR-M category remained negatively associated with survival independently of histopathologic features. Although the recent study by Centonze et al (31) did not identify any prognostic value in LI-RADS categories compared with microvascular invasion and satellite nodules, that study excluded all HCCs categorized as LR-M. In a separate study of patients with single and multifocal HCC, the performance of a preoperative score based on clinical, laboratory, and radiologic variables was found to be similar to that of a postoperative score that included histopathologic features of the tumor (32). Overall, our results confirm that the LR-M category should be considered in addition to pathology.

One major finding of our study is the association between nontargetoid features (ie, infiltrative appearance, marked diffusion restriction, and necrosis or severe ischemia) and the risk of recurrence, independently of the LI-RADS category. This was confirmed after matching patients for medical center, size greater than 50 mm, LI-RADS high-risk status, satellite nodules, micro- and macrovascular invasion, World Health Organization grade, and LI-RADS category. Nontargetoid features were frequent in our study sample, as at least one nontargetoid feature was observed in 94.7% and 87.5% of patients at CT and MRI, respectively. Of note, only a minority of HCCs with at least one

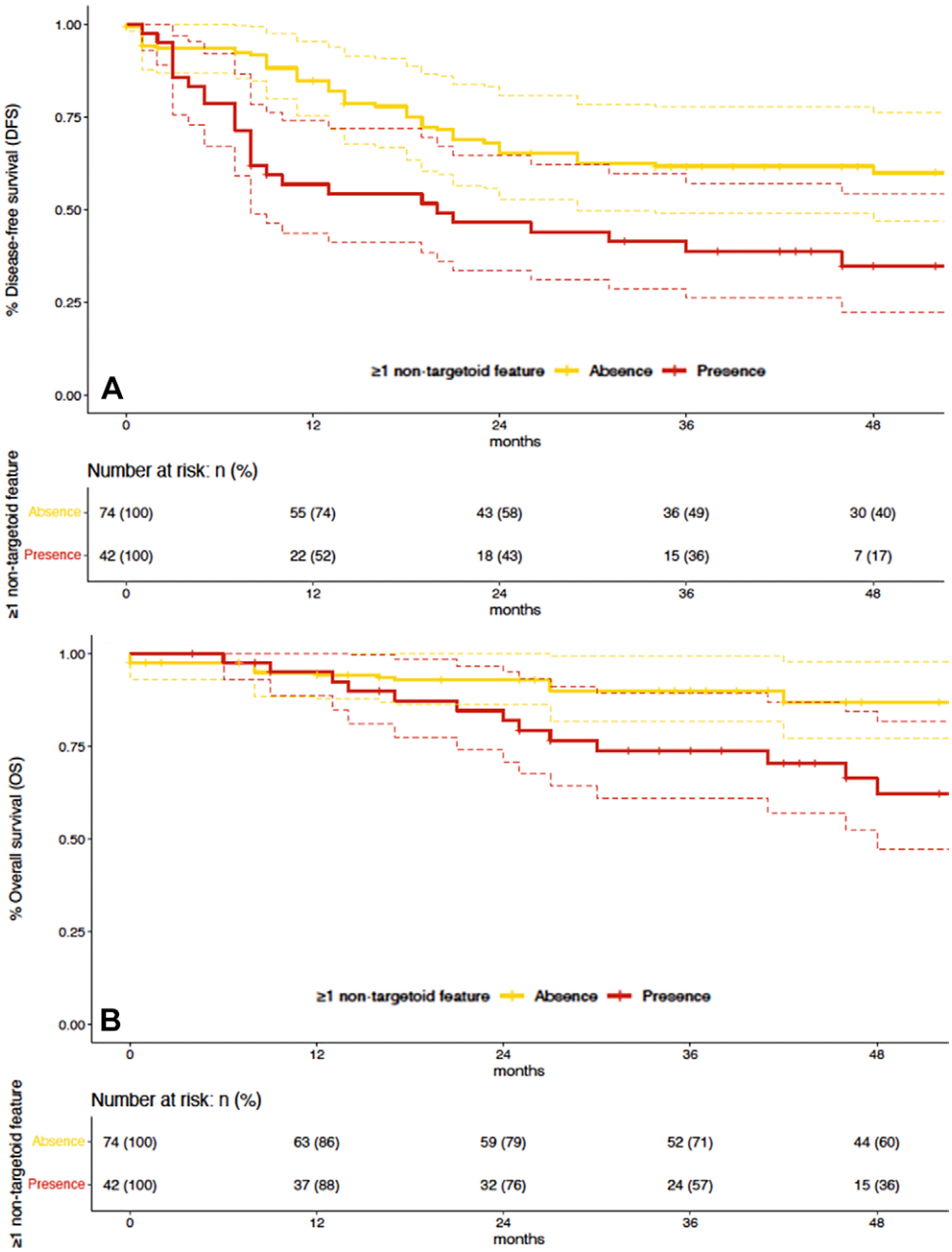

Figure 5: Graphs show Kaplan-Meier curves for **(A)** disease-free survival (DFS) and **(B)** overall survival (OS) in patients with CT examinations according to the presence of at least one nontargetoid feature after matching *(Fig 5 continues)*.

nontargetoid feature were classified as LR-M (12.4% and 15.6% at CT and MRI, respectively), and most were categorized as LR-5 (67.4% and 70.1% at CT and MRI, respectively). Evidence supporting the prognostic value of nontargetoid features per se is scarce. Several studies have shown that most macrotrabecular-massive HCCs—a proliferative subgroup, often with poor prognosis—are categorized as LR-5 but frequently contain necrosis or ischemia (19,33). Overall, our study shows that nontargetoid features are frequent, underrecognized, yet important prognostic features worth considering in refining LI-RADS as a prognostic tool (especially for LR-5 observations).

The interreader agreement was moderate to substantial for the presence of at least one LR-M feature, major features, and LI-RADS categories, which is consistent with the agreement values reported in recent meta-analyses (34,35). However, despite intermodality differences between CT and MRI in the percentage of enhancing "capsule," fat sparing in solid mass, fat in mass, and blood products in mass, LR-M category and the presence of at least one nontargetoid feature were associated with survival and risk of recurrence for both modalities.

This study has several limitations. First, while the multicenter design improves the generalizability of the results, the imbalance in caseload between the enrolled centers must be taken into consideration. Second, retrospective assessment of histopathologic data from different pathologists without a centralized review precluded any measurement

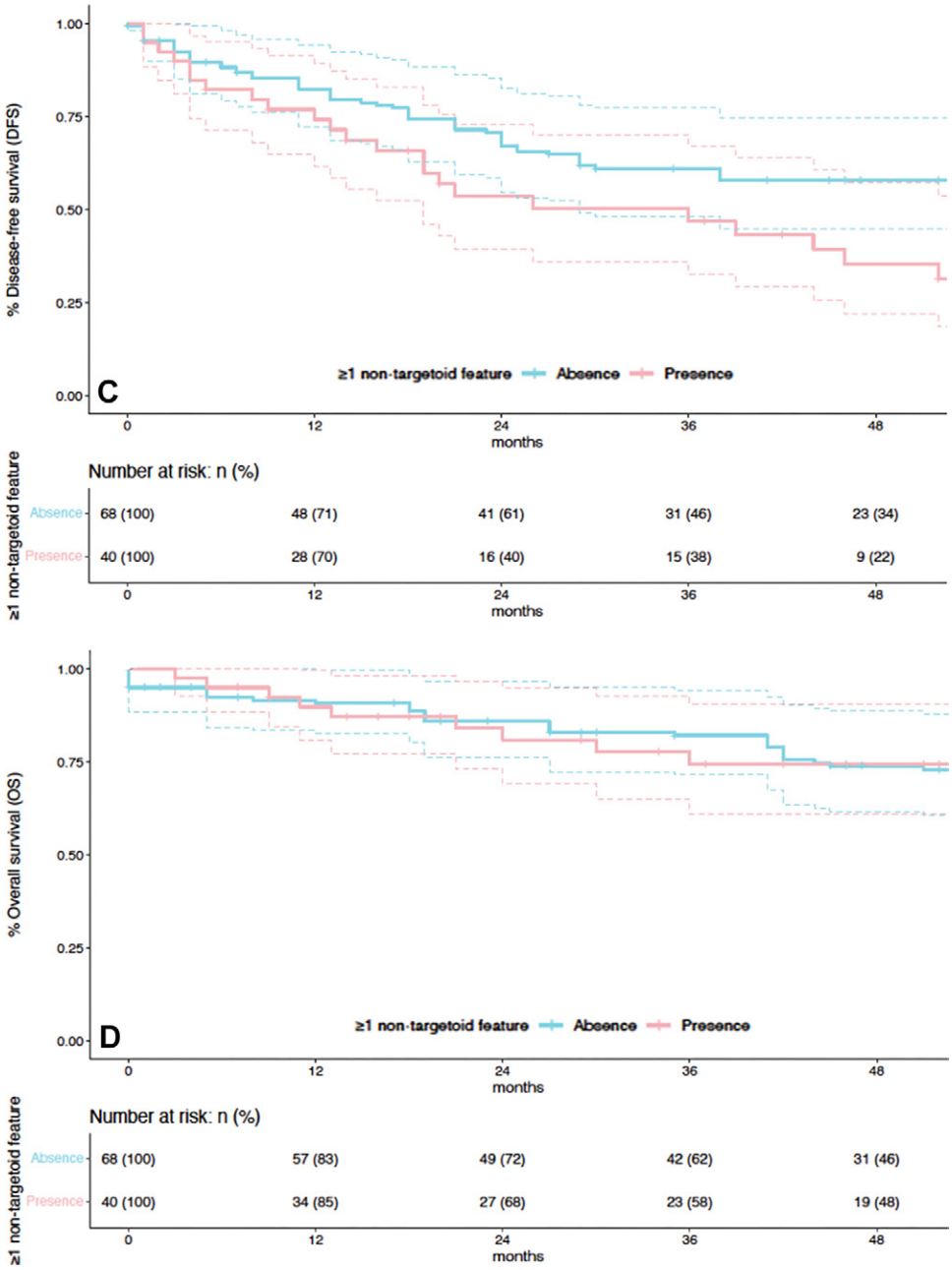

Figure 5 *(continued).* Graphs show Kaplan-Meier curves for **(C)** DFS and **(D)** OS in patients with MRI examinations according to the presence of at least one nontargetoid feature after matching.

of the agreement between different pathologists. Third, this study did not consider HCC subtypes (because subtype data were available from only one center) or the vessels encapsulating tumor clusters pattern, which are also associated with poor survival in patients with HCC (33,36). Finally, observations were collected over a period of 12 years with different scanners and contrast agents, although all the imaging examinations were acquired in accordance with LI-RADS technical recommendations.

In conclusion, Liver Imaging Reporting and Data System (LI-RADS) LR-M category at CT or MRI was associated with decreased disease-free and overall survival in patients with solitary hepatocellular carcinoma undergoing resection. Additionally, the presence of at least one nontargetoid feature was independently associated with increased recurrence risk, regardless of LI-RADS category, and should be carefully reported.

Author contributions: Guarantors of integrity of entire study, **A. Laurent, V.V., F.C., M.R.**; study concepts/study design or data acquisition or data analysis/interpretation, all authors; manuscript drafting or manuscript revision for important intellectual content, all authors; approval of final version of submitted manuscript, all authors; agree to ensure any questions related to the work are appropriately resolved, all authors; literature research, **R.C., F.M., J.C., S.M., E.R., A. Laurent, O. Scatton, F.C., M.R.**; clinical studies, **F.M., R.S., A.B., S.M., A. Luciani, A. Laurent, M.W., O. Scatton, M.R.**; statistical analysis, **R.C., C.H., M.R.**; and manuscript editing, **R.C., F.M., M.D.B., R.S., A.B., J.C., S.M., A. Luciani, A. Laurent, O. Seror, N.G.C., M.W., O. Scatton, V.V., F.C., C.H., M.R.**

Disclosures of conflicts of interest: **R.C.** Co-funding from the European Union—FESR or Fonds Social Européen, Programme Opérationnel National Research and Innovation 2014–2020 (DM 1062/2021); research collaboration with Siemens Healthineers; and support for attending meetings and/or travel from Bracco and Bayer. **F.M.** No relevant relationships. **M.D.B.** No relevant relationships. **R.S.** No relevant relationships. **A.B.** No relevant relationships. **J.C.** No relevant relationships. **S.M.** No relevant relationships. **E.R.** No relevant relationships. **A. Luciani** Research grant for Consortium Multitechnologique pour le Diagnostic Précoce et l'Amélioration du Traitement du CHC/Artificial Intelligence for Diagnostic, Review and Radiomics Acceleration in Medicine research project from GE HealthCare, consulting fees from Guerbet, payment for teaching webinar from Bracco, support for attending GE user meeting (October 2023) from GE HealthCare, general secretary of the French Society of Radiology. **A. Laurent** No relevant relationships. **O. Seror** No relevant relationships. **N.G.C.** Payment or honoraria for lectures, presentations, speakers bureaus, manuscript writing, or educational events from AbbVie, Gilead, and Roche and support for attending meetings and/or travel from Gilead. **M.W.** Payment for lectures from Bracco and support for attending meetings and/or travel from Bayer. **O. Scatton** No relevant relationships. **V.V.** No relevant relationships. **F.C.** No relevant relationships. **C.H.** No relevant relationships. **M.R.** Consulting fees from Quantum Surgical and payment or honoraria for lectures, presentations, speakers bureaus, manuscript writing, or educational events from Ispen, Guerbet, Servier, General Electric, AngioDyamics, and AstraZeneca.

References

1. Cerny M, Bergeron C, Billiard JS, et al. LI-RADS for MR imaging diagnosis of hepatocellular carcinoma: performance of major and ancillary features. Radiology 2018;288(1):118–128.
2. Kim YY, Kim MJ, Kim EH, Roh YH, An C. Hepatocellular carcinoma versus other hepatic malignancy in cirrhosis: performance of LI-RADS version 2018. Radiology 2019;291(1):72–80.
3. CT/MRI LI-RADS v2018 core. American College of Radiology. https://www.acr.org/-/media/ACR/Files/RADS/LI-RADS/LI-RADS-2018-Core.pdf. Posted 2018. Accessed March 20, 2023.
4. Marrero JA, Kulik LM, Sirlin CB, et al. Diagnosis, staging, and management of hepatocellular carcinoma: 2018 practice guidance by the American Association for the Study of Liver Diseases. Hepatology 2018;68(2):723–750.
5. Tanabe M, Kanki A, Wolfson T, et al. Imaging outcomes of Liver Imaging Reporting and Data System version 2014 category 2, 3, and 4 observations detected at CT and MR imaging. Radiology 2016;281(1):129–139.
6. Choi SH, Byun JH, Lim YS, et al. Liver Imaging Reporting and Data System: patient outcomes for category 4 and 5 nodules. Radiology 2018;287(2):515–524.
7. Hong CW, Park CC, Mamidipalli A, et al. Longitudinal evolution of CT and MRI LI-RADS v2014 category 1, 2, 3, and 4 observations. Eur Radiol 2019;29(9):5073–5081.
8. Wei H, Yang T, Chen J, Duan T, Jiang H, Song B. Prognostic implications of CT/MRI LI-RADS in hepatocellular carcinoma: state of the art and future directions. Liver Int 2022;42(10):2131–2144.
9. European Association for the Study of the Liver. EASL clinical practice guidelines: management of hepatocellular carcinoma. J Hepatol 2018;69(1):182–236. [Published correction appears in J Hepatol 2019;70(4):817.]
10. Portolani N, Coniglio A, Ghidoni S, et al. Early and late recurrence after liver resection for hepatocellular carcinoma: prognostic and therapeutic implications. Ann Surg 2006;243(2):229–235.
11. An C, Park S, Chung YE, et al. Curative resection of single primary hepatic malignancy: Liver Imaging Reporting and Data System category LR-M portends a worse prognosis. AJR Am J Roentgenol 2017;209(3):576–583.
12. Choi SH, Lee SS, Park SH, et al. LI-RADS classification and prognosis of primary liver cancers at gadoxetic acid-enhanced MRI. Radiology 2019;290(2):388–397.
13. Shin J, Lee S, Kim SS, et al. Characteristics and early recurrence of hepatocellular carcinomas categorized as LR-M: comparison with those categorized as LR-4 or 5. J Magn Reson Imaging 2021;54(5):1446–1454.
14. Moon JY, Min JH, Kim YK, et al. prognosis after curative resection of single hepatocellular carcinoma with a focus on LI-RADS targetoid appearance on preoperative gadoxetic acid-enhanced MRI. Korean J Radiol 2021;22(11):1786–1796.
15. Imamura H, Matsuyama Y, Tanaka E, et al. Risk factors contributing to early and late phase intrahepatic recurrence of hepatocellular carcinoma after hepatectomy. J Hepatol 2003;38(2):200–207.
16. Roayaie S, Obeidat K, Sposito C, et al. Resection of hepatocellular cancer ≤2 cm: results from two Western centers. Hepatology 2013;57(4):1426–1435.
17. Lee EC, Kim SH, Park H, Lee SD, Lee SA, Park SJ. Survival analysis after liver resection for hepatocellular carcinoma: a consecutive cohort of 1002 patients. J Gastroenterol Hepatol 2017;32(5):1055–1063.
18. Fowler KJ, Burgoyne A, Fraum TJ, et al. Pathologic, molecular, and prognostic radiologic features of hepatocellular carcinoma. RadioGraphics 2021;41(6):1611–1631.
19. Cannella R, Dioguardi Burgio M, Beaufrère A, et al. Imaging features of histological subtypes of hepatocellular carcinoma: Implication for LI-RADS. JHEP Rep 2021;3(6):100380.
20. Kambadakone AR, Fung A, Gupta RT, et al. LI-RADS technical requirements for CT, MRI, and contrast-enhanced ultrasound. Abdom Radiol (NY) 2018;43(1):56–74. [Published correction appears in Abdom Radiol (NY) 2018;43(1):240.]
21. WHO Classification of Tumours Editorial Board. Digestive system tumours. In: WHO classification of tumours. 5th ed. Lyon, France: International Agency for Research on Cancer, 2019; 229–239.
22. Bedossa P, Poynard T. An algorithm for the grading of activity in chronic hepatitis C. The METAVIR Cooperative Study Group. Hepatology 1996;24(2):289–293.
23. Kleiner DE, Brunt EM, Van Natta M, et al. Design and validation of a histological scoring system for nonalcoholic fatty liver disease. Hepatology 2005;41(6):1313–1321.
24. Benchoufi M, Matzner-Lober E, Molinari N, Jannot AS, Soyer P. Interobserver agreement issues in radiology. Diagn Interv Imaging 2020;101(10):639–641.
25. Austin PC. The performance of different propensity score methods for estimating marginal hazard ratios. Stat Med 2013;32(16):2837–2849.
26. Daniel R, Zhang J, Farewell D. Making apples from oranges: comparing noncollapsible effect estimators and their standard errors after adjustment for different covariate sets. Biom J 2021;63(3):528–557.
27. Borgan Ø. Modeling survival data: extending the Cox model. Springer-Verlag, New York, 2000. No. of pages: xiii + 350. Price: $69.95. ISBN 0-387-98784-3. Stat Med 2001;20(13):2053–2054.
28. Austin PC. The use of propensity score methods with survival or time-to-event outcomes: reporting measures of effect similar to those used in randomized experiments. Stat Med 2014;33(7):1242–1258.
29. Ho D, Imai K, King G, Stuart EA. MatchIt: nonparametric preprocessing for parametric causal inference. J Stat Softw 2011;42(8):1–28.
30. Hong SB, Choi SH, Kim SY, et al. MRI features for predicting microvascular invasion of hepatocellular carcinoma: a systematic review and meta-analysis. Liver Cancer 2021;10(2):94–106.
31. Centonze L, De Carlis R, Vella I, et al. From LI-RADS classification to HCC pathology: a retrospective single-institution analysis of clinicopathological features affecting oncological outcomes after curative surgery. Diagnostics (Basel) 2022;12(1):160.
32. Wei H, Jiang H, Qin Y, et al. Comparison of a preoperative MR-based recurrence risk score versus the postoperative score and four clinical staging systems in hepatocellular carcinoma: a retrospective cohort study. Eur Radiol 2022;32(11):7578–7589.
33. Mulé S, Galletto Pregliasco A, Tenenhaus A, et al. Multiphase liver MRI for identifying the macrotrabecular-massive subtype of hepatocellular carcinoma. Radiology 2020;295(3):562–571.
34. Kang JH, Choi SH, Lee JS, et al. Interreader agreement of liver imaging reporting and data system on MRI: a systematic review and meta-analysis. J Magn Reson Imaging 2020;52(3):795–804.
35. Kang JH, Choi SH, Lee JS, et al. Inter-reader reliability of CT Liver Imaging Reporting and Data System according to imaging analysis methodology: a systematic review and meta-analysis. Eur Radiol 2021;31(9):6856–6867. [Published correction appears in Eur Radiol 2021;31(11):8820–8821.]
36. Feng Z, Li H, Zhao H, et al. Preoperative CT for characterization of aggressive macrotrabecular-massive subtype and vessels that encapsulate tumor clusters pattern in hepatocellular carcinoma. Radiology 2021;300(1):219–229.